Received February 1997
Revised November 1997
Accepted December 1997

Free convection in vertical eccentric annuli with a uniformly heated boundary

Maged A.I. El-Shaarawi and Esmail M. A. Mokheimer
Mechanical Engineering Department, King Fahd University of Petroleum and Minerals, Dhahran, Saudi Arabia

Nomenclature

a = location of the positive pole of the bipolar coordinate system on the x-axis, equal $r_i \ Sinh \ \eta$i or $r_o \ Sinh \ \eta_o$

a* = local heat transfer coefficient, $q''/(T_w - T_o)$

$\bar{a}$ = average heat transfer coefficient over annulus height, $\int_0^1 a^* dZ/l$

A = cross-sectional area of the channel, $\pi(r_o^2 - r_i^2)$

c_p = specific heat of fluid at constant pressure

D_h = equivalent (hydraulic) diameter of annulus, $2(r_o - r_i) = 2a(1 - N) \ Csch \ \eta_o$

e = eccentricity (distance between the two centers of the two cylinders forming the eccentric annulus), $a(Coth \ \eta_o - Coth \ \eta_i)$

E = dimensionless eccentricity (dimensionless center-to-center distance), $e/(r_o - r_i)$

$$= \frac{Sinh(\eta_i - \eta_O)}{Sinh \ \eta_i - Sinh \ \eta_o}$$

f = volumetric flow rate, $f = \int_{ri}^{ro} 2\pi r u dr = \pi(r_o^2 - r_i^2)\bar{u} = 2\int_0^{\pi}\int_{\eta o}^{\eta i} uh^2 d\eta d\xi$

F = dimensionless volumetric flow rate, $f/\pi l \gamma Gr^* = 8(1 - N)2\int_0^{\pi}\int_{\eta o}^{\eta i} U H^2 \, d\eta d\xi/\pi$

g = gravitational body force per unit mass(acceleration)

Gr = Grashof number, $\pm g\beta q'' D_h^4/2\gamma^2 k$, the plus and minus signs apply to upward (heating) and downward (cooling) flows, respectively. Thus Gr is always positive

Gr* = modified Grashof number, $Gr^* = Gr \ D_h/l$

h = coordinate transformation scale factor, $a(Cosh \ \eta - Cos \ \xi)$

H = dimensionless coordinate transformation factor,

$$h/D_h = \frac{0.5Sinh(\eta_o)}{(1-N)(Cosh(\eta) - (Cos(\xi))}$$

i = index of the numerical grid in η-direction

j = index of the numerical grid in ξ-direction

k = thermal conductivity of fluid

l = height of annulus

L = dimensionless height of annulus (value of Z at annulus exit), 1/ Gr*

m = number of steps of the numerical grid in ξ-direction

n = number of steps of the numerical grid in the η-direction or infinite – series summation parameter in analytical solution

n* = direction normal to either boundary and the direction of positive q''

N = annulus radius ratio, r_i/r_o = Sinh η_o/Sinh η_i

p = pressure of fluid inside the channel at any cross-section

p′ = pressure defect at any point, $p - p_s$

p_o = pressure of fluid at annulus entrance

p_s = hydrostatic pressure, $\mp \rho_o g z$ where the minus and plus signs are for upward (heating) and downward (cooling) flows respectively

P = dimensionless pressure defect at any point, $p' D_h^4/\rho_o l^2 \gamma^2 Gr^{*2}$

Pr = Prandtl number, $\mu \ c_p/k$

q'' = local heat flux at either boundary which is defined to be positive when it heats the fluid, $-k\partial T/\partial n\bullet = \pm (k/h)(\partial T/\partial \eta)$ where the upper and lower signs stand for the inner and outer walls respectively, in case of fluid heating and vice versa in case of fluid cooling

International Journal of Numerical Methods for Heat & Fluid Flow
Vol. 8 No. 5, 1998, pp. 488–503.

Esmail M.A. Mokheimer is on leave from Ain Shams University, Cairo, Egypt.

The support of King Fahd University of Petroleum and Minerals (KFUPM) to carry out this investigation is gratefully acknowledged.

q = heat gained or lost by fluid from the entrance up to a particular elevation in the annulus, $\rho_o f c_p (T_m - T_o)$

$\bar{q}$ = heat gained or lost by fluid from the entrance up to the annulus exit, i.e., value of q at $z = l$, $\rho_o f c_p (\bar{T}_m - T_o)$

Q = dimensionless heat absorbed from the entrance up to any particular elevation, $q/[\pi\rho_o c_p l\gamma Gr^* (T_w - T_o)] = F\theta_m$

$\bar{Q}$ = dimensionless heat absorbed up to the annulus exit, i.e. value of Q at $z = l$, $\bar{q}/[\pi\rho_o c_p l\gamma Gr^*(T_w - T_o)] = F\bar{\theta}_m$

r_i = inner radius of annulus

r_o = outer radius of annulus

Ra = Rayleigh number, Gr Pr

Ra* = modified Rayleigh number, $Gr^* Pr = Ra\, D_h/l$

T = temperature at any point

T_m = mixing-cup (mixed-mean or fluid-bulk) temperature over any cross-section at a given z, $\int_A Tu dA/(A\bar{u}) = 2\int_0^{\pi}\int_{\eta_o}^{\eta_i} Tuh^2 d\eta d\xi / [\pi(r_0^2 - r_i^2)\bar{u}]$

$\bar{T}_m$ = mixing cup temperature at annulus exit, i.e. value of T_m at $z = l$

T_w = temperature of isothermal wall

u = axial (streamwise) velocity component at any point

u_o = entrance axial velocity, $\bar{u}$

$\bar{u}$ = average u (volume flow rate per unit area), $\int u dA / A =$ $2\int_0^{\pi}\int_{\eta_o}^{\eta_i} uh^2 d\eta d\xi/[\pi r_o^2 - r_i^2)\bar{u}] =$ $2\int_0^{\pi}\int_{\eta_o}^{\eta_i} uh^2 d\eta d\xi/[\pi a^2(1 - N^2) Csch^2\eta_o \bar{u}]$

U = dimensionless axial velocity at any point, $\frac{ur_o^2}{l\gamma Gr^*}$

$\bar{U}$ = dimensionless average axial velocity at any point, $\frac{ur_o^2}{l\gamma Gr^*}$

x = the first transverse direction in the Cartesian coordinate system

y = the second transverse direction in the Cartesian coordinate system

z = axial coordinate in both the Cartesian and bipolar coordinate systems

Z = dimensionless axial coordinate, $z / l\, Gr^*$

Greek letters:

β = volumetric coefficient of thermal expansion

η = the first transverse bipolar coordinate

η_i = value of η on the inner surface of the annulus, given by equation (1)

η_o = value of η on the outer surface of the annulus, given by equation (2)

$\Delta\eta$ = numerical grid mesh size in η-direction, $(\eta_i - \eta_o) / n$

θ = dimensionless temperature,

θ_m = dimensionless mixed-mean temperature,

$\bar{\theta}_m$ = dimensionless mixed-mean temperature at channel exit,

μ = dynamic viscosity of fluid

ξ = the second transverse bipolar coordinate

$\Delta\xi$ = numerical grid mesh size in ξ-direction, π/m

ρ_o = fluid density at ambient temperature

ϕ = normalized value of η, $(\eta - \eta_o)/(\eta_i - \eta_o)$

ψ = normalized value of ξ, ξ/π

Introduction

Having many practical applications, laminar free or forced convection with simultaneously developing hydrodynamic and thermal boundary layers in vertical annuli has received a great deal of attention. Such type of heat transfer may exist in vertical electric motors and generators and in atomic reactors. Most of the work available in the literature deals with concentric annuli. However, in many practical situations eccentricities might be introduced in nominally concentric annuli as a result of manufacturing tolerances or operating conditions.

Fully developed forced flow and convection heat transfer in eccentric annuli have been tackled by some investigators. Heyda[1] determined the Green's function in bipolar coordinates for the potential flow in an eccentric annulus and then solved the momentum equation for the velocity profile. Snyder[2] utilized the analytical solution obtained by El-Saden[3] for the conduction heat transfer problem to solve the differential equation describing the slug flow heat transfer in an eccentric annulus. Using the same technique, Snyder and

Goldstein[4] obtained the fully developed velocity profile for laminar forced flow in eccentric annuli. However, Redberger and Charles[5] solved the same problem numerically by means of finite-difference techniques and bipolar coordinates. Using cylindrical coordinates, Cheng and Hwang[6] and Trombetta[7] obtained approximate solutions for the energy equation under different boundary conditions in the case of fully developed laminar forced flow in eccentric annuli.

A very thorough literature survey has revealed that only two papers, by Feldman *et al.*[8,9], are available for the investigation of developing forced convection in eccentric annuli. In these two papers, the two transverse momentum equations were dropped. Consequently, the hydrodynamic model comprised only two equations, namely, a reduced axial momentum equation and the continuity equation. However, since there are three unknown components of the velocity in addition to the pressure, this two-equation model required additional assumptions regarding the transverse flows to facilitate a solution.

No work has been found in the literature dealing with free convection in open-ended vertical eccentric annuli. However, the developing laminar free convection in open-ended vertical concentric annuli has been studied by El-Shaarawi and Sarhan[10] and Al-Arabi *et al.*[11]. El-Shaarawi and Al-Nimr[12] presented analytical solutions for the fully developed free convection in open-ended concentric annuli. Four pairs of fundamental boundary conditions, as defined by Reynolds *et al.*[13], were investigated. These fundamental boundary conditions are obtained by combining each of the two conventional boundary conditions of having one boundary at constant heat flux or at constant temperature with each of the conditions wherein the opposite boundary is kept either isothermal at the inlet fluid temperature or adiabatic. Fully developed free convection in open-ended vertical annuli is the limiting case for the more general problem of developing free convection in such channels. In the latter case fully developed conditions can be achieved if the annulus is sufficiently high or, more general, if the Rayleigh number has a sufficiently low value.

The first objective of the present paper is to present a boundary-layer model for the problem of natural convection heat transfer in vertical eccentric annuli. The second objective is to develop a numerical algorithm to solve the obtained model. Finally, numerical results are presented for the velocity profiles, axial variation of pressure, heights required to suck specified flow rates, and heat transfer parameters under the thermal boundary conditions obtained by having one of the annulus boundaries at a constant heat flux while the other boundary is maintained at the ambient temperature T_o.

Governing equations and method of solution

A two-dimensional cross-section plan and elevation of the geometry under consideration are shown in Figure 1(a). This eccentric geometry can easily be described by the bipolar coordinate system (η, ξ and z) shown in Figure 1(b).

The transformation equations from the Cartesian coordinate system (x, y and z) to this bipolar system are given in the nomenclature. In this orthogonal coordinate system the two cylindrical boundaries of the annulus coincide with two surfaces having constant values of η (η_i and η_o, which can be expressed in terms of the annulus radius ratio N and the dimensionless eccentricity E as given in the nomenclature). The other coordinate (ξ) represents a set of eccentric cylinders whose centres lie on the y-axis and which orthogonally intersect the boundaries of the annulus. The transformed geometry in the complex $\eta - \xi$ plane is, for a given value of z, a slab of length ($\eta_i - \eta_o$) and width equal to the limits of ξ, that is 2π.

The vertical eccentric annulus of finite length shown in Figure 1(a) is open at both ends and is immersed in a stagnant Newtonian fluid of infinite extent maintained at constant temperature T_o. Free convection flow is induced inside this annular channel as a result of heating or cooling one of its vertical walls at a uniform heat flux while keeping the other wall at the ambient temperature T_o. Thus, two cases are under investigation, namely, case (I) in which the heat transfer boundary is the inner wall and case (O) in which the

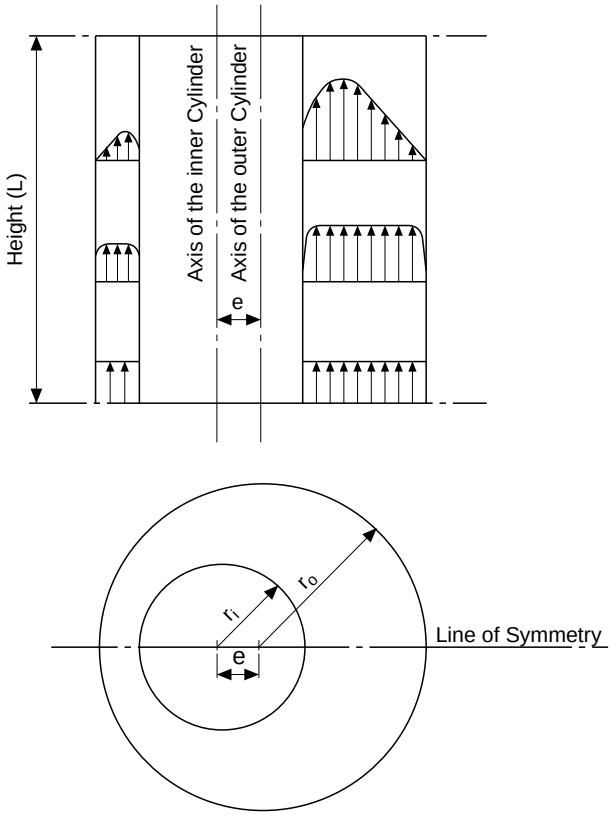

Figure 1(a). Two-dimensional elevation and plan for the geometry under consideration

heat transfer boundary is the outer wall of the annulus. The fluid enters the channel at the ambient temperature T_0 and is assumed to have constant physical properties but obeys the Boussinesq approximation according to which its density is allowed to vary with temperature in only the gravitational body force term of the vertical (axial) momentum equation. Thus Boussinesq approximation neglects the compressibility effect everywhere except for the buoyancy force term. Body forces in other than the vertical direction, viscous dissipation, internal heat generation, and radiation heat transfer are absent (Figure 1(b)).

The governing equations in a general orthogonal curvilinear coordinate system are given in two references (Hughes and Gaylord[14] and Moon and Spencer[15]). Using the appropriate coordinate scale factors[14]), the governing equations in bipolar coordinates under the above mentioned assumptions are as follows:

Continuity equation

$$\frac{\partial(hw)}{\partial\xi}+\frac{\partial(hv)}{\partial\eta}+\frac{\partial(h^2u)}{\partial z}=0 \tag{1}$$

ξ – *Momentum equation*

$$\rho\left(\frac{w}{h}\frac{\partial w}{\partial\xi}+\frac{v}{h^2}\frac{\partial hw}{\partial\eta}+u\frac{\partial w}{\partial z}-\frac{v^2}{h^2}\frac{\partial h}{\partial\xi}\right)=-\frac{1}{h}\frac{\partial p}{\partial\xi}+\frac{\mu}{h}\left(\begin{array}{l}\dfrac{\partial^2(hw)}{\partial z^2}+\dfrac{1}{h^2}\dfrac{\partial^2(hw)}{\partial\eta^2}+\dfrac{1}{h^2}\dfrac{\partial^2(hw)}{\partial\xi^2}\\ +\dfrac{2}{h^3}\left(\dfrac{\partial(hv)}{\partial\xi}-\dfrac{\partial(hw)}{\partial\eta}\right)\dfrac{\partial h}{\partial\eta}+\dfrac{2}{h^2}\dfrac{\partial h}{\partial\xi}\dfrac{\partial hu}{\partial z}\end{array}\right) \tag{2}$$

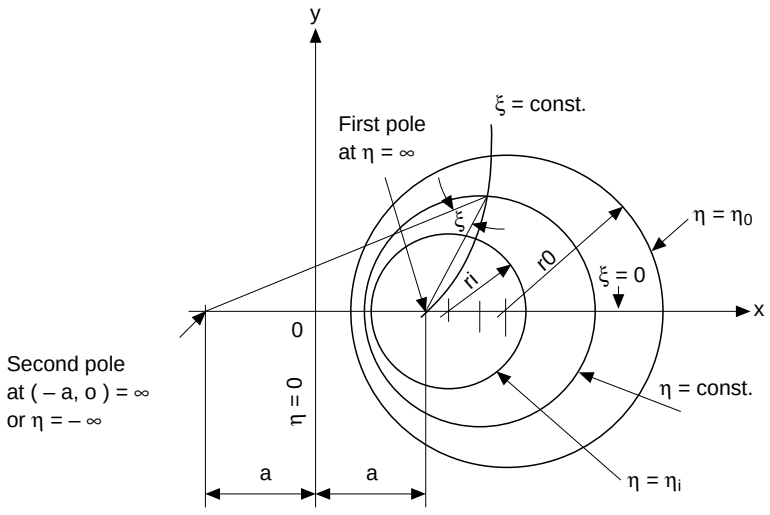

Figure 1(b).
Bipolar coordinate system

η – *Momentum equation*

$$\rho\left(\frac{w}{h^2}\frac{\partial hv}{\partial \xi}+\frac{v}{h}\frac{\partial v}{\partial \eta}+u\frac{\partial v}{\partial z}-\frac{w^2}{h^2}\frac{\partial h}{\partial \eta}\right)=-\frac{1}{h}\frac{\partial p}{\partial \eta}+\frac{\mu}{h}\left(\begin{array}{l}\dfrac{\partial^2(hv)}{\partial z^2}+\dfrac{1}{h^2}\dfrac{\partial^2(hv)}{\partial \eta^2}+\dfrac{1}{h^2}\dfrac{\partial^2(hv)}{\partial \xi^2}\\ -\dfrac{2}{h^3}\left(\dfrac{\partial(hv)}{\partial \xi}-\dfrac{\partial(hw)}{\partial \eta}\right)\dfrac{\partial h}{\partial \xi}+\dfrac{2}{h^2}\dfrac{\partial h}{\partial \eta}\dfrac{\partial hu}{\partial z}\end{array}\right) \quad (3)$$

z – *Momentum equation*

$$\rho\left(\frac{w}{h}\frac{\partial u}{\partial \xi}+\frac{v}{h}\frac{\partial u}{\partial \eta}+u\frac{\partial u}{\partial z}\right)=F_z-\frac{\partial P}{\partial z}+\frac{\mu}{h^2}\left(h^2\frac{\partial^2 u}{\partial z^2}+\frac{\partial^2 u}{\partial \eta^2}+\frac{\partial^2 u}{\partial \xi^2}\right) \quad (4)$$

Energy equation

$$\rho c_p\left(\frac{w}{h}\frac{\partial T}{\partial \xi}+\frac{v}{h}\frac{\partial T}{\partial \eta}+u\frac{\partial T}{\partial z}\right)=\frac{k}{h^2}\left(h^2\frac{\partial^2 T}{\partial z^2}+\frac{\partial^2 T}{\partial \eta^2}+\frac{\partial^2 T}{\partial \xi^2}\right) \quad (5)$$

The differential continuity equation (1) subject to the no slip conditions on the two boundaries can be written in the following integral form:

$$\pi(r_o^2-r_i^2)\bar{u}=2\int_0^{\pi}\int_{\eta_o}^{\eta_i}h^2\,u\,d\xi\,d\eta \quad (6)$$

Some parabolic-flow assumptions[16] will be used to simplify the above model. These assumptions include: the pressure is a function of the axial coordinate only ($\partial p/\partial\eta = \partial p/\partial\xi = 0$), the axial diffusions of momentum and energy are neglected ($\partial^2/\partial z^2 = 0$), and the η- velocity component (v) is much smaller than the ξ- and z-velocity components (w and u). Introducing the dimensionless parameters given in the nomenclature and taking into consideration that the latter assumption results in dropping the η-momentum equation, equations (1) through (6) can be replaced by the following five dimensionless equations:

$$\frac{\partial(HW)}{\partial \xi}+\frac{\partial(HV)}{\partial \eta}+4(1-N)^2\frac{\partial(H^2U)}{\partial Z}=0 \quad (7)$$

$$\frac{W}{H}\frac{\partial W}{\partial \xi}+\frac{V}{H^2}\frac{\partial HW}{\partial \eta}+4(1-N)^2U\frac{\partial W}{\partial Z}-\frac{V^2}{H^2}\frac{\partial H}{\partial \xi}=\frac{1}{H^3}\left(\frac{\partial^2 HW}{\partial \eta^2}+\frac{\partial^2 HW}{\partial \xi^2}\right)$$
$$-\frac{2}{H^4}\left(\frac{\partial HW}{\partial \eta}-\frac{\partial HV}{\partial \xi}\right)\frac{\partial H}{\partial \eta}+\frac{8(1-N)^2}{H^2}\frac{\partial H}{\partial \xi}\frac{\partial U}{\partial Z} \quad (8)$$

$$\frac{W}{H}\frac{\partial U}{\partial \xi}+\frac{V}{H}\frac{\partial U}{\partial \eta}+4(1-N)^2U\frac{\partial U}{\partial Z}=-\frac{1}{4(1-N)^2}\frac{dP}{dZ}+\frac{\theta}{4(1-N)^2}+\frac{1}{H^2}\left[\frac{\partial^2 U}{\partial \xi^2}+\frac{\partial^2 U}{\partial \eta^2}\right] \quad (9)$$

$$\frac{W}{H}\frac{\partial \theta}{\partial \xi}+\frac{V}{H}\frac{\partial \theta}{\partial \eta}+4(1-N)^2U\frac{\partial \theta}{\partial Z}=\frac{1}{Pr.H^2}\left(\frac{\partial^2 \theta}{\partial \xi^2}+\frac{\partial^2 \theta}{\partial \eta^2}\right) \quad (10)$$

$$\bar{U}=\frac{8(1-N)}{\pi(1+N)}\int_0^{\pi}\int_{\eta_o}^{\eta_i}U\,H^2\,d\eta\,d\xi \quad (11)$$

Equations (7) through (10) are subject to the following boundary conditions:

$$\left.\begin{array}{l} \text{for } Z=0 \text{ and } \eta_o<\eta<\eta_i,\ V=W=\theta=0 \text{ and } U=U_o,\ P=-U_o^2/2 \\ \\ \text{for } Z\geq 0 \text{ and } \eta=\eta_i,\ U=V=W=0,\ \partial\theta/\partial\eta\big|_{\eta_i}=\pm H(\eta_i,\xi) \text{ for case (I) or } \theta=0 \text{ for case (O)} \\ \text{for } Z\geq 0 \text{ and } \eta=\eta_o,\ U=V=W=0,\ \partial\theta/\partial\eta\big|_{\eta_o}=\mp H(\eta_o,\xi) \text{ for case (O) or } \theta=0 \text{ for case (I)} \\ \\ \text{for } Z\geq 0 \text{ and } \xi=0 \text{ and } \pi \text{ (the line of symmetry)}: \\ \dfrac{\partial V}{\partial \xi}=\dfrac{\partial W}{\partial \xi}=\dfrac{\partial U}{\partial \xi}=\dfrac{\partial \theta}{\partial \xi}=0 \\ \\ \text{for } Z=L \text{ and } \eta_o\leq\eta\leq\eta,\ P=0 \end{array}\right\} \quad (12)$$

Equations (7) through (11) were written in linearized finite-difference forms and then numerically solved[17]. Owing to symmetry, the above equations need to be solved in only half of the slab , i.e. for $0 \leq \xi \leq \pi$.

In practice, for confined free convection flows the dimensions of the channel (l and D) and both the wall conditions and ambient temperature are normally known (i.e. L is given) while the volumetric flow rate f (and hence F) is unknown. However, the present model and method of solution are handling the problem in a reversed manner, i.e. obtaining an unknown dimensionless channel height (L) for a given dimensionless volumetric flow rate (F). Therefore, the condition $P = 0$ at $Z = L$ is not explicitly imposed on the solution, but continually checked for satisfaction; recall that the governing equations (8-10) are parabolic in Z and need only one condition with respect to Z.

All results to be presented in this paper have been obtained using a grid of 20 segments in the η-direction and 20 segments in the ξ-direction. Thus, for each axial step, 400 ($19 \times 21 + 1 = 399 + 1$) equations have to be solved to obtain the values of U and P then 399 equations have to be solved for W and 420 equations for θ, according to the thermal boundary conditions considered. This required about 35 CPU seconds per one axial step on a main frame computer of WF 77 sys D type. Moreover, the results to be presented here have been obtained by using very small axial steps near the entrance ($\Delta Z = 10^{-10}$ for all the cases considered) then the axial step was increased several times as the flow moves downstream to reach a value no more than $\Delta Z = 10^{-3}$.

The mesh size (20×20) has been chosen after some numerical experimentation. In these preliminary numerical experiments, different mesh sizes (10×10, 15×15, 20×20 and 25×25) have been tested. The impact of the mesh size on the channel height required for case (I) to suck a flow with $U_o = 0.001$ in a channel of $E = 0.7$ has been analysed. The results of this analysis proved that the refinement of the grid from 20×20 to 25×25 has an effect of about 2 per cent only on the channel height. Other numerical tests with mesh sizes of 30×30 indicated that the corresponding computer CPU time would be considerably increased and such tests were not finalised owing to some limitations.

Results and discussion

Owing to the neglect of the axial diffusion ($\partial^2/\partial Z^2 = 0$) and variations of pressure with the two transverse directions ($\partial P/\partial \eta = \partial P/\partial \xi = 0$), the Grashof number is inherent in the dimensionless formulation of the problem and thus it is not explicitly needed for the solution. However, four other similarity parameters are explicitly required to solve the problem under consideration. These are the annulus radius ratio (N), the dimensionless eccentricity (E), the dimensionless flow rate F (or effectively $U_0 = F / (1 - N^2)$) and the Prandtl number (Pr). However, one should recall that the inlet velocity (U_0) and hence the inlet pressure (P_0) and the volumetric flow rate (F) are not predetermined initial conditions independent of the channel height as in the case of forced flows. Rather, each of them is dependent on the channel height and the applied heat flux on the heat transfer wall. Moreover, since one of the annulus' two boundaries is maintained isothermal, there is, as was explained by El-Shaarawi and Al-Nimr[12], an upper limiting value for U_0 for each value of N and E ($U_{0,fd}$). These upper limiting values can be obtained by analytically solving the fully- developed energy equation for θ_{fd} then these solutions for θ_{fd} are substituted in a finite-difference form of the fully-developed momentum equation to numerically obtain the fully-developed velocity profiles U_{fd}. For given N and E, the average value of the corresponding U_{fd}-profile gives the required upper limiting value ($U_{0,fd}$) and its corresponding value of the volumetric flow rate ($F_{fd} = U_{0,fd}/(1- N^2)$). For a wide range of E =0.1-0.9, these upper limiting values can be found in Mokheimer[17].

Computations were carried out for a fluid of Pr = 0.7 in an annulus of N = 0.5. The radius ratio 0.5 was chosen since it represents a typical annular geometry with its value of N far enough from unity (N = 1) which represents the case of a parallel plate channel. Moreover, the free convection results in concentric annuli of El-Shaarawi and Sarhan[10] are for this particular radius ratio (N = 0.5). These results provided a means of verification of the present algorithm and the computer code through special runs at a very small eccentricity ($E = 10^{-6}$) under thermal boundary conditions of one wall being isothermal while the opposite is adiabatic. This very low value of $E = 10^{-6}$ was used rather than E = 0.0 since the latter can not be used for computations in bipolar coordinates as it represents a singularity for transformation from the Cartesian to bipolar coordinates.

Owing to space limitations, only a representative sample of the results will be presented. Figure 2(a) shows examples of the developing axial velocity profiles in the widest and narrowest sides of the gap of an annulus of $N = E = 0.5$ under thermal boundary condition (I) for a uniform inlet velocity $U_0 = 4.35 \times 10^{-3}$. This inlet velocity corresponds to a flow rate $F = 3.2625 \times 10^{-3}$ which is very near to the fully developed flow rate[17] ($F_{fd} = 3.301 \times 10^{-3}$). Similar results for case (O) are given in Figure 2(b) corresponding to an inlet velocity of 17.1×10^{-3} (which is corresponding to a flow rate of 0.012825 and is very near to the fully developed flow rate F_{fd} = 0.012867). It can be seen from these two Figures that, very near to the entrance (e.g. profiles 1,2 and 3), the fluid decelerates near the two walls of the

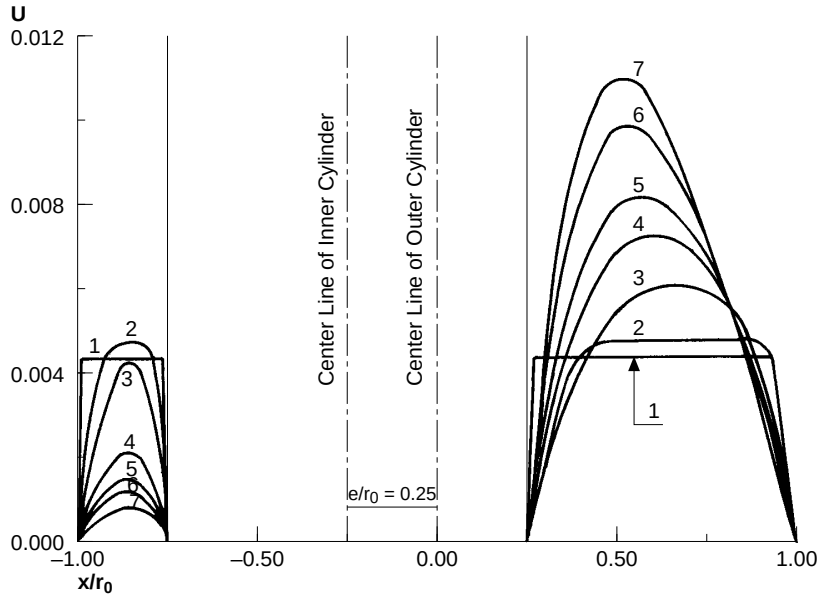

Figure 2(a). Development of the axial velocity profiles, $N = E = 0.5$, case (I), $U_0 \times 10^3 = 4.35$. The numbers on the profiles indicate the following values of $Z \times 10^7$: (1) 10^{-3}, (2) 21.8, (3)212, (4)712, (5)1,212, (6) 3,112, (7) 13,112 (and above, until full development)

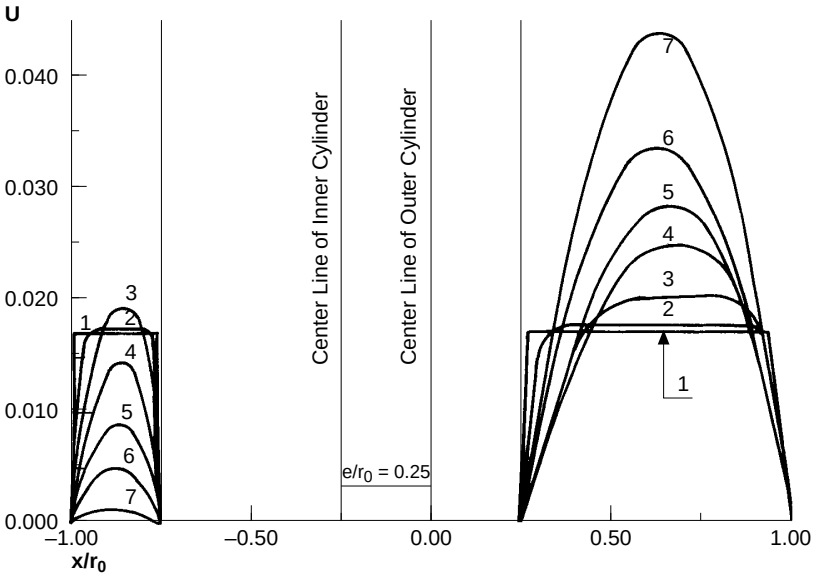

Figure 2(b). Development of the axial velocity profiles, $N = E = 0.5$, case (O), $U_0 \times 10^3 = 17.1$. The numbers on the profiles indicate the following values of $Z \times 10^7$: (1) 10^{-3}, (2) 21.8, (3)212, (4)712, (5)1,212, (6) 3,112, (7) 13,112 (and above, until full development)

annulus owing to the formation of the two boundary layers on the walls and accelerates in the core region as a result of the continuity principle. However, further downstream, since the eccentricity increases/decreases the resistance to flow on the narrowest/widest gap side of the annulus, the axial velocity profile develops with increasing/decreasing values on the widest/narrowest gap side of

the annulus as the flow moves away from the entrance. Such a development continues until U reaches its invariant fully-developed axial-velocity profile (U_{fd}), since the channel is high enough in these two presented cases. Also, it has been found that the developing temperature profiles(unpresented in the paper) reach their fully-developed distribution θ_{fd}. This provided a check on the adequacy of the present computer code.

For given N and E, the channel height required to naturally induce a specific flow rate is one of the important engineering parameters. For a given F, this height can be determined by monitoring the value of the pressure as the flow moves away from the entrance of the channel till the dimensionless pressure becomes zero. Examples of the axial variation of the dimensionless pressure in an annulus of E = 0.1 are presented in Figure 3. This figure shows that, for a given U_0 (i.e. a given F), the inlet negative pressure ($P_0 = -U_0^2/2$) decreases due to friction as the flow moves up in the annulus until a minimum value is attained. It then increases due to buoyancy until the dimensionless pressure becomes zero at the channel exit. Thus, the negative pressure gradient increases until it reaches a zero value at the axial location where the buoyancy force becomes equal to the friction force then it becomes a positive pressure gradient due to the increase in the buoyancy force resulting from the heating

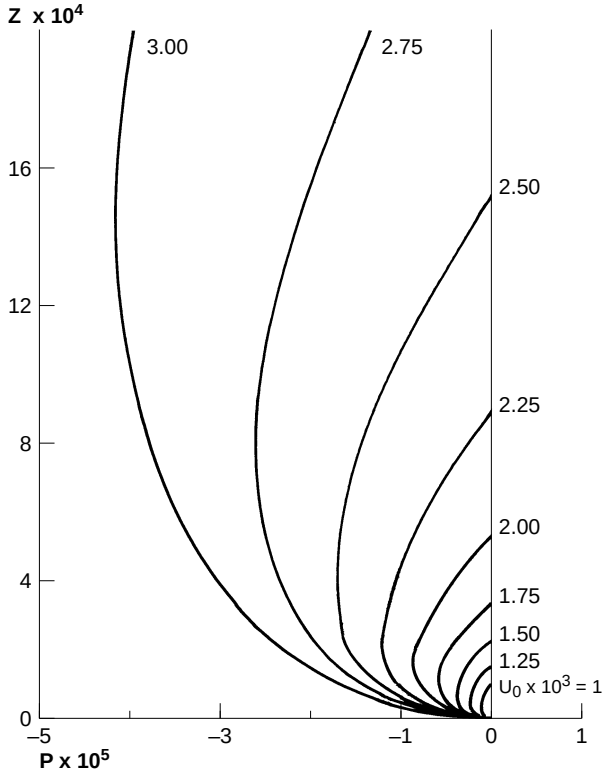

Figure 3. Development of the pressure with Z for different values of the induced volumetric flow rate (i.e. different channel heights), N = 0.5, E = 0.7, case (I)

effect. The point at which the dimensionless pressure becomes zero determines the channel height and the figures show that the channel height increases as the required induced flow rate increases (i.e. as U_0 increases). However, for the present cases with one isothermal boundary there is an upper limit for U_0 (= $U_{0,fd}$) beyond which there will be no more increase in the induced flow rate regardless of the channel height.

The variation of the induced flow rate with the channel height is shown in Figures 4(a) and 4(b) for cases (I) and (O) respectively. In these two figures, results are presented for three values of E (0.1, 0.5 and 0.7). It is clear from these figures that, for given N and E, the required channel height to suck up a specific dimensionless flow rate is larger for case (I) than for case (O). This is attributed to the larger heating surface in case (O) than in case (I). Another observation from Figures 4(a) and 4(b) is that increasing the eccentricity E causes an increase in F in both cases (I) and (O). This qualitatively agrees with the trend of the reported forced-flow results in the literature which indicate that increasing E reduces the resistance to flow.

For cases (I) and (O) respectively, Figures 5(a) and 5(b) give the variation of the heat gained by the fluid from entrance up to the annulus exit ($\bar{Q}$) with the

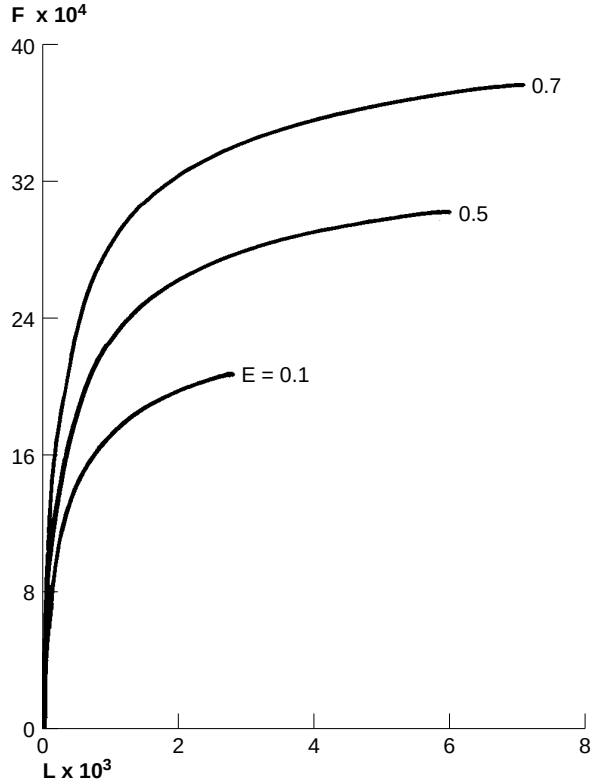

Figure 4(a).
The induced volumetric flow rate versus channel height, for various values of E, N = 0.5, case (I)

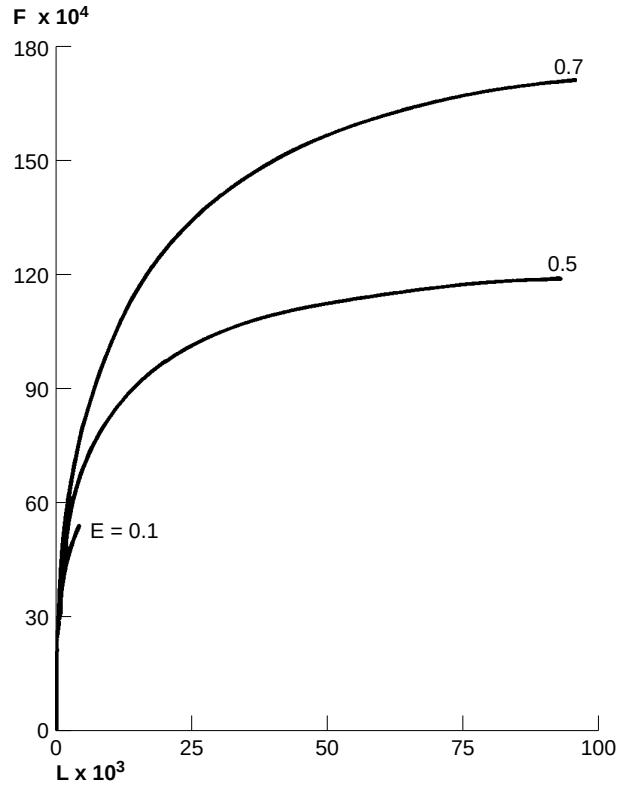

Figure 4(b). The induced volumetric flow rate versus channel height, for various values of E, N = 0.5, case (O)

channel height L for the three dimensionless eccentricities investigated. These figures show that, for a given annulus (i.e. given N, L and E), the higher the value of the eccentricity the larger the total heat absorbed by the fluid. This is attributed to the increase in the flow rate with eccentricity as was clarified in Figures 4(a) and 4(b).

The variation of the dimensionless mixing-cup (mixed-mean) temperature θ_m with Z, for various values of U_0 (i.e. various values of F or, implicitly, L) and both boundary conditions considered, is shown in Figures 6(a) through 6(c) for the three considered values of eccentricity, namely, E = 0.1, 0.5 and 0.7 respectively. In each of these figures, curves corresponding to three values (low, intermediate and high) of U_0 are drawn for each boundary condition. Note that for small values of U_0 (i.e. F), the curves are shown up to the axial distance at which the pressure defect reached a zero value (i.e. the exit cross-section). It is clear from these figures that θ_m for thermal boundary condition (O) is greater than that for thermal boundary condition (I) at same Z and F in a given annulus. Again this is due to the larger heating surface in case (O) than that in case (I). On the other hand, with large values of U_0 (i.e. near enough to $U_{0,fd}$) the value of θ_m for either boundary condition attains its fully developed value (which is

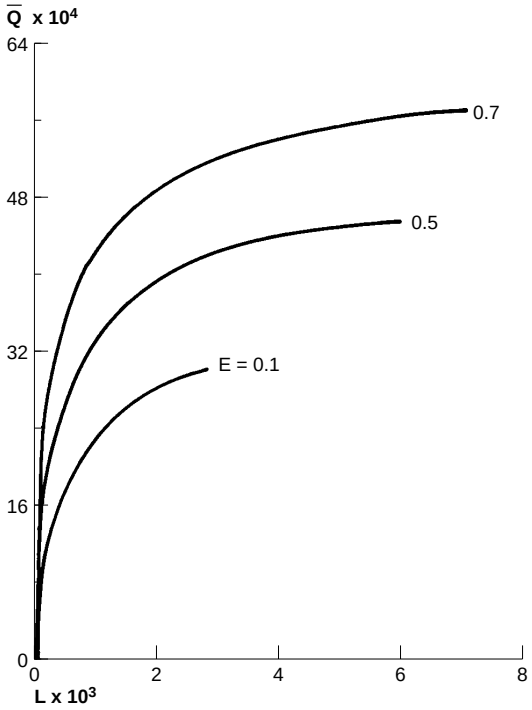

Figure 5(a).
The total heat absorbed by the fluid against the channel height for various eccentricities, N = 0.5, case (I)

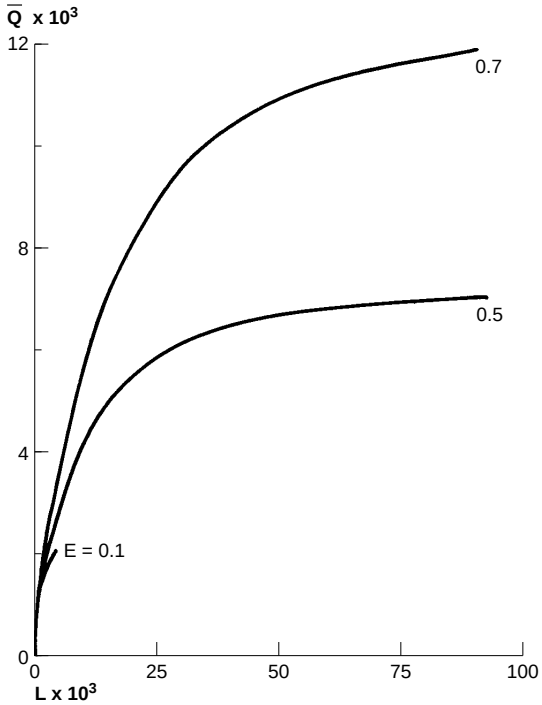

Figure 5(b).
The total heat absorbed by the fluid against the channel height for various eccentricities, N = 0.5, case (O)

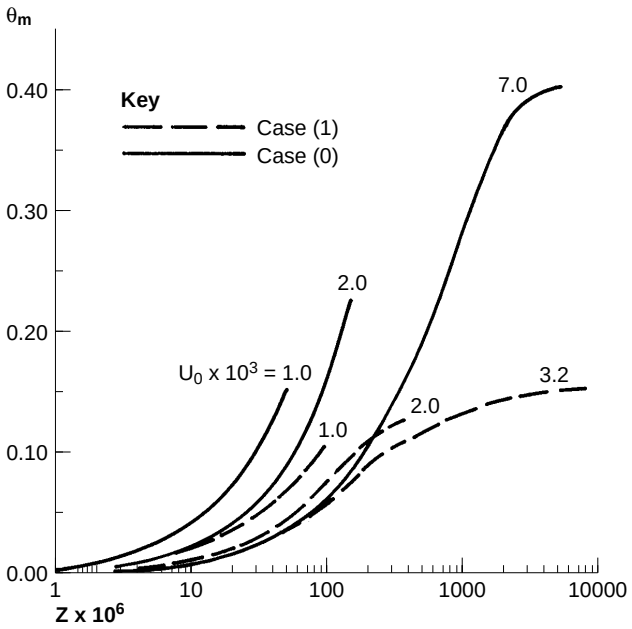

Figure 6(a).
Variation of θ_m with Z for various values of U_o, $N = 0.5$, $E = 0.1$

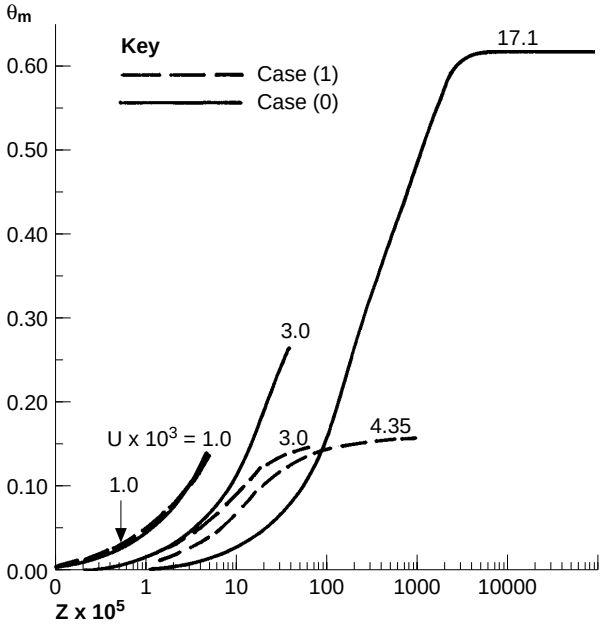

Figure 6(b).
Variation of θ_m with Z for various values of U_o, $N = 0.5$, $E = 0.5$

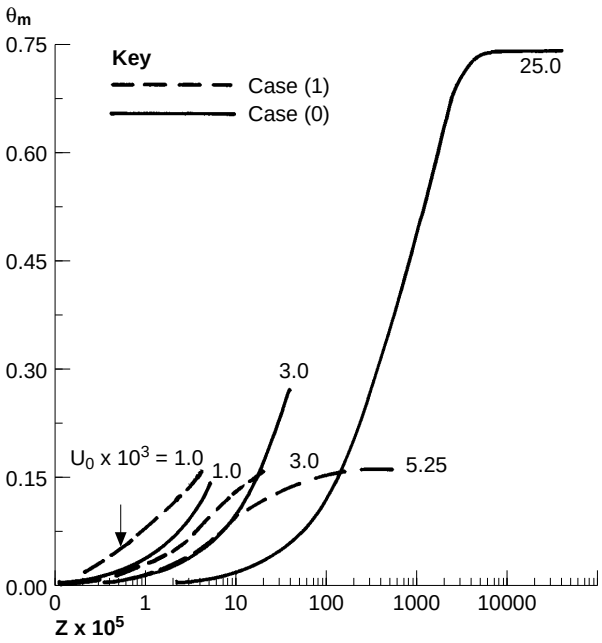

Figure 6(c).
Variation of θ_m with Z for various values of U_o, $N = 0.5$, $E = 0.7$

invariant with Z) before the fluid reaches the annulus top exit. In other words, the flow reaches the state of thermal full development before it becomes hydrodynamically fully developed. This is a feature of natural convection flows in channels, regardless of the value of Pr, as was explained by El-Shaarawi and Al-Nimr[12]. When thermal full development is reached, the θ-profile does not vary with further increase in Z. In the present case, under these fully-developed conditions, the heat passes from the heated wall to the opposite cooled wall (which is maintained at T_0) by pure conduction through laminar layers, i.e. as if the fluid were stationary.

Conclusions

A parabolic-flow model in bipolar coordinates has been presented for the developing laminar free convection in open-ended vertical eccentric annuli. A linearized finite-difference algorithm has been developed to numerically solve this model. Numerical results are presented for a fluid of $Pr = 0.7$ in an annulus of radius ratio 0.5. Three values of dimensionless eccentricity and two thermal boundary conditions have been investigated. These thermal boundary conditions are obtained by having one of the annulus walls uniformly heated while the opposite wall is isothermally cooled and maintained at the inlet-fluid (ambient) temperature.

The results show that both the induced flow rate and the total heat absorbed by the fluid increase with eccentricity. The variations of the induced flow rate and the total heat absorbed by the fluid with the channel height have been

presented for use in practical applications. Finally, the obtained results also show that heating the outer boundary of the annulus is more useful for inducing flow (thermosyphons) than heating its inner boundary.

References

1. Heyda, J.F., "A Green's function solution for the case of laminar incompressible flow between non-concentric cylinders", *J. Franklin Inst.,* Vol. 267, 1959, pp. 25-34.
2. Snyder, W.T., "An analysis of slug flow heat transfer in an eccentric annulus", *A.I.Ch.E. Journal,* Vol. 9 No. 4, 1963, pp. 503-6.
3. El-Saden, M.R., "Heat conduction in an eccentrically hollow, infinitely long cylinder with internal heat generation", *J. Heat Transfer,* Vol. 83 No. 4, 1961, pp. 510-11.
4. Snyder, W.T. and Goldstein, G.A., "An analysis of a fully developed laminar flow in an eccentric annulus", *A.I.Ch.E. Journal,* Vol. 11 No. 3, 1965, pp. 462-9.
5. Redberger, P.J. and Charles, M.E., "Axial laminar flow in a circular pipe containing a fixed eccentric core", *The Canadian Journal of Chemical Engineering,* Vol. 40, 1962, pp. 148-51.
6. Cheng, K.C. and Hwang, G.J., "Laminar forced convection in eccentric annuli", *A.I.Ch.E. Journal,* Vol. 14 No. 3, 1968, pp. 510-12.
7. Trombetta, M.L., " Laminar forced convection in eccentric annuli", *Int. J. Heat Mass Transfer,* Vol. 14, 1972, pp. 1161-72.
8. Feldman, E.E., Hornbeck, R.W. and Osterle, J.F., "A numerical solution of laminar developing flow in eccentric annular ducts", *Int. J. Heat Mass Transfer,* Vol. 25 No. 2, 1982, pp. 231-41.
9. Feldman, E.E., Hornbeck, R.W. and Osterle, J.F., "A numerical solution of developing temperature for laminar developing flow in eccentric annular ducts", *Int. J. Heat Mass Transfer,* Vol. 25 No. 2, 1982, pp. 243-53, 11 A1-10.
10. El-Shaarawi, M.A.I. and Sarhan, A., "Developing laminar free convection in an open ended vertical annulus with a rotating inner cylinder", *J. Heat Transfer,* Vol. 103, 1981, pp. 552-8.
11. Arabi, M., El-Shaarawi, M.A.I. and Khamis, M., "Natural convection in uniformly heated vertical annuli", *Int. J. Heat Mass Transfer,* Vol. 30 No. 7, 1987, pp. 1381-9.
12. El-Shaarawi, M.A.I. and Al-Nimr, M.A., "Fully developed laminar natural convection in open-ended vertical concentric annuli", *Int. J. Heat and Mass Transfer*, Vol. 33 No. 9, 1990, pp. 1873-84.
13. Reynolds, W.C., Lundberg, R.E. and McCuen, P.A., "Heat transfer in annular passages. General formulation of the problem for arbitrarily prescribed wall temperatures or heat fluxes", *Int. J. Heat Mass Transfer,* Vol. 6, 1963, pp. 483-93. Carnahan, B., Luther, H. A., and Wilkes, J. D., *Applied Numerical Methods,* Wiley, 1969, pp. 298-301, 450.
14. Hughes, W.F. and Gaylord, E.W., *Basic Equations of Engineering Science,* Schaum's outline series, McGraw Hill, New York, 1964, pp. 1-11, 151.
15. Moon, P. and Spencer, D.E., *Field Theory Handbook,* 2nd ed., Springer Verlag, Berlin, 1971, pp. 1-5.
16. Schlichting, H., *Boundary Layer Theory,* 7th ed., McGraw-Hill, New York, 1987, pp. 127-49.
17. Mokheimer, E.M.A., "Heat transfer in eccentric annuli", PhD dissertation, Mechanical Engineering Department, King Fahd University of Petroleum and Minerals (KFUPM), Dhahran, Saudi Arabia.